Lab on a Chip

View Online
Dynamic Article Links

Cite this: *Lab Chip*, 2011, **11**, 147

www.rsc.org/loc

PAPER

Self-assembled magnetic filter for highly efficient immunomagnetic separation†

David Issadore,[a] Huilin Shao,[a] Jaehoon Chung,[a] Andita Newton,[a] Mikael Pittet,[a] Ralph Weissleder[ab] and Hakho Lee*[a]

Received 27th June 2010, Accepted 14th September 2010
DOI: 10.1039/c0lc00149j

We have developed a compact and inexpensive microfluidic chip, the self-assembled magnetic filter, to efficiently remove magnetically tagged cells from suspension. The self-assembled magnetic filter consists of a microfluidic channel built directly above a self-assembled NdFeB magnet. Micrometre-sized grains of NdFeB assemble to form alternating magnetic dipoles, creating a magnetic field with a very strong magnitude B (from the material) and field gradient ∇B (from the configuration) in the microfluidic channel. The magnetic force imparted on magnetic beads is measured to be comparable to state-of-the-art microfabricated magnets, allowing for efficient separations to be performed in a compact, simple device. The efficiency of the magnetic filter is characterized by sorting non-magnetic (polystyrene) beads from magnetic beads (iron oxide). The filter enriches the population of non-magnetic beads to magnetic beads by a factor of $>10^5$ with a recovery rate of 90% at 1 mL h^{-1}. The utility of the magnetic filter is demonstrated with a microfluidic device that sorts tumor cells from leukocytes using negative immunomagnetic selection, and concentrates the tumor cells on an integrated membrane filter for optical detection.

Introduction

The efficient separation and enrichment of targeted cells from a heterogeneous suspension is a crucial task in medical and biological sciences, with applications in cancer diagnostics,[1,2] drug discovery,[3] and stem cell research.[4] Magnetic separation of cells has emerged as a promising alternative and supplement to conventional fluorescence activated cell sorting (FACS).[5] Immunomagnetic sorting can be performed on inexpensive, easy to use, bench-top equipment, in contrast to FACS which requires trained personnel, a dedicated lab space, and a considerable capital cost.[6] Another key advantage for magnetic sorting is that it can process many cells in parallel, enabling high throughput operations compared to FACS that processes cells one at a time ($<10^8$ cells per hour).[6] This feature is especially important for isolating rare cells, such as circulating tumor cells and endothelial cells from a vast background of host cells.[7,8]

Much work has been done to develop and improve tools for magnetic separation. Magnetic sorting was first used to isolate red blood cells (RBCs) from whole blood using a high gradient magnetic field filter[9] and the intrinsic magnetic properties of RBCs.[10] With the development of monoclonal antibodies, the technique was extended to immunomagnetic separation wherein nonmagnetic cells are labeled with magnetic particles coated with antibodies specific to targeted biomarkers.[6,11] Magnetic sorters have been improved through the application of microfabrication.[12–17] Using lithography, magnetic field profiles can be engineered by patterning current carrying wires[14,18] and ferromagnetic materials.[13,15] Using microfluidics, bifurcated laminar flows have been used in conjunction with magnetic separation to increase sorting efficiency.[12,13,15–17,19] Magnetic sorters that require microlithography cannot be manufactured using extremely inexpensive techniques such as injection molding. More so than the cost of fabrication, the requirements of external plumbing, electronics, and optics have limited the use of these microfluidic devices as a disposable point-of-care tool.

Here we report the development of a new magnetic separation system that increases sorting efficiency, simplifies use, and can be manufactured at a very low cost. The key innovation is the self-assembled magnetic layer which produces a magnetic field $\boldsymbol{B}$ with large strength ($B = |\boldsymbol{B}|$) and gradients (∇B), and thus imparts strong magnetic forces [$\sim(\boldsymbol{B}\cdot\nabla)\boldsymbol{B}$] on cells (see ESI†). As a proof-of-concept, we have implemented a prototype system consisting of a microfluidic channel built directly above a layer of NdFeB grains, the strongest known permanent magnetic material.[20] The self-assembled magnet produced with NdFeB, create magnetic forces that are comparable to state of the art microfabricated magnets.[21] The strong magnetic force enables highly

[a]*Center for Systems Biology, Massachusetts General Hospital, 185 Cambridge St, CPZN 5206, Boston, MA, 02114, USA*
[b]*Department of Systems Biology, Harvard Medical School, 200 Longwood Av, Alpert 536, Boston, MA, 02115, USA. E-mail: hlee@mgh.harvard.edu; Fax: +1617-643-6133; Tel: +1 617-643-0500*

† Electronic supplementary information (ESI) available: Theoretical description and numerical simulations of the self-assembled magnetic filter. See DOI: 10.1039/c0lc00149j

efficient cell separation, enriching magnetic species from nonmagnetic ones by a factor of $>10^5$. The self-assembled magnetic filter is compact and simple to use, eliminating the need for complex, external microfluidic components (*e.g.* pumps). The self-assembled magnetic filter is cost-effective for disposable uses as it requires only a single external pump, no lithography for fabrication, and uses inexpensive material. Thus, the self-assembled magnetic filter can be a practical tool for point-of-care applications.

Methods

The design of the self-assembled magnetic filter is inspired by the operation of micro-electromagnetic mirrors used in atomic physics.[22] These mirrors consist of arrays of magnetic dipoles arranged in alternating directions (Fig. 1a). The configuration creates field patterns that decay exponentially in space, generating a large field gradient ∇B. Here, the same principle is applied to the arrangement of highly magnetic material to achieve both large magnetic field strength B (from the material) and magnetic field gradient ∇B (from the configuration). In implementing such a system, we employ the self-assembly of magnetic material: permanently magnetized materials tend to form antiparallel configuration of moments to minimize magnetic energy (Fig. 1b).

The length-scale of the magnetic field gradient can be controlled by choosing the size of the magnetic grains. The strength of the magnetic force $[\sim(\boldsymbol{B}\cdot\nabla)\boldsymbol{B}]$ above a two dimensional array of alternating dipoles, using the coordinates shown in Fig. 1a, can be expressed in an analytical form[23] (see ESI†):

$$\left|(\vec{B}\cdot\vec{\nabla})\vec{B}\right| = \sum_{k,l} F_{k,l} e^{-2\pi|z|\sqrt{(k/a)^2+(l/b)^2}} \qquad (1)$$

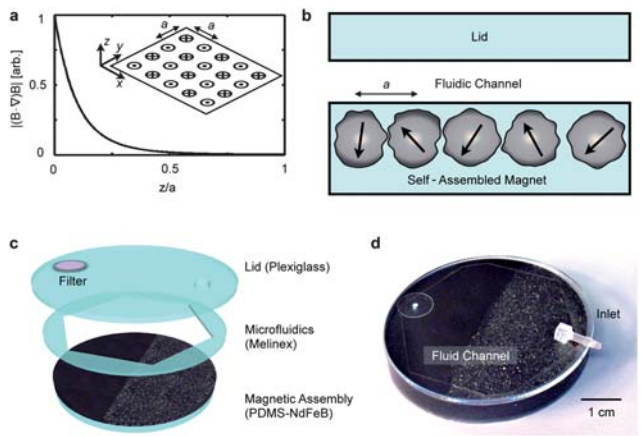

Fig. 1 Self-assembled magnetic filter creates very large magnetic force $[\sim(\boldsymbol{B}\cdot\nabla)\boldsymbol{B}]$ to efficiently remove magnetically tagged objects from suspensions. (a) Magnet design. Alternating magnetic dipoles create a magnetic field that decays rapidly in distance. (b) When magnetic materials are allowed to self-assemble, the magnetic moments align into a similar configuration as in (a). This self-assembled layer produces a very strong magnetic field and field gradient. (c) A prototype self-assembled magnetic filter was fabricated that consists of self-assembled layers of 125 μm grain (right) and 8 μm grain (left) permanent magnetic material (NdFeB) with a microfluidic channel built directly on top. A micropore filter is placed on the output to collect and concentrate the cells that are negatively enriched by the self-assembled magnet. (d) A photograph of the prototype.

where a is the pitch between magnetic dipoles, $F_{k,l}$ are the Fourier components of magnetic field, and k and l are the indices for the Fourier components of the field. The Fourier components vanish and the magnetic field $\boldsymbol{B}$ goes to zero far from the array. Using this relationship, the strength of the magnetic field gradient and the distance that the gradient extends from the magnet, can be traded-off and engineered for specific applications.

To demonstrate the technique of using self-assembled magnets, we have fabricated a prototype self-assembled magnetic filter (Fig. 1c) consisting of a self-assembled layer of permanent magnets integrated below a microfluidic channel. To implement the self-assembled magnet, we first magnetized NdFeB powder (Magnequench) suspended in uncured PDMS (polydimethylsiloxane) using a high-field magnet (>1 T). Subsequently, the mixture was slowly cured (>1 hour) to allow for the self-assembly of NdFeB grains. A microfluidic channel was then built directly on top of the cured magnet using a 50 μm thick layer of two-sided adhesive coated polyester film (Melinex, DuPont). The channel patterns were defined *via* laser-cutting (VLS3, VersaLaser) for fast prototyping. A lid was constructed using 1.5 mm thick extruded poly(methyl methacrylate) sheet (Plexiglas, McMaster Carr), with holes for the input and output defined with the laser cutter. Additionally, a membrane filter with 5 μm pores (Nuclepore, Whatman) was sealed over the output hole using a layer of laser-cut polyester film. The membrane filter captured cells for optical inspection after the magnetic separation step. Fig. 1d shows a photograph of a prototype self-assembled magnetic filter system. The device has two magnetic sections for efficient cell capture. At the entry port, the self-assembled magnetic layer is made of 125 μm grains of NdFeB (MQP-B-20076, Magnequench). The layer creates a magnetic field that extends throughout the channel height, pulling the cells towards the bottom of the channel. Further along the channel, the grain size was reduced to 8 μm (MQFP-B-20076, Magnequench) to create a stronger, but more short range force to firmly trap cells (eqn (1)).

To evaluate the capability of the self-assembled magnetic filter for cell sorting, we performed a negative enrichment of tumor cells suspended in an abundant population of leukocytes. The samples were prepared by mixing a known amount of leukocytes and tumor cells. Leukocytes were harvested from a mouse spleen by dissociating the tissue followed by RBC lysis. Tumor cells (SK-BR-3, breast carcinoma) were cultured in McCoy's medium, supplemented with fetal bovine serum (FBS, 10%), penicillin and streptomycin (1%), L-glutamine (1%), and maintained at 37 °C in a humidified atmosphere containing 5% of CO_2.

For quantitative analysis of cell separation by the self-assembled magnetic filter, we performed flow cytometry on samples before and after sorting. Leukocytes were stained green with CFSE (carboxyfluorescein succinimidyl ester, Invitrogen). Briefly, the cells ($\sim10^7$ mL^{-1}) were incubated at room temperature with 1 μM CFSE for 10 min. The incubation was stopped with 100% FBS and the cells were triple-washed before spiking with tumor cells. SK-BR-3 cells ($\sim10^6$ mL^{-1}) were stained with 1 μM CellTracker Red CMPTX (Invitrogen). The two cell populations were mixed at different ratios and incubated with CD45 magnetic beads (MACS, Miltenyi Biotec) at 4 °C for specific labeling of leukocytes. The cell mixtures were subsequently fixed in formaldehyde and pumped through the

self-assembled magnetic filter using a syringe pump (BS8000, Braintree Scientific).

The utility of the self-assembled magnetic filter as a practical tool to remove specific cells from a background population for optical inspection is demonstrated using a microfluidic device with an integrated membrane filter to concentrate targeted cells. In this operation, the population of leukocytes and tumor cells was concurrently labeled in a single incubation step. Samples were prepared by mixing leukocytes (pre-stained with CFSE) and SK-BR-3 cells at different ratios. The cell mixtures were then incubated simultaneously with CD45 magnetic beads to specifically target leukocytes and fluorescently labeled HER2/*neu* antibodies (Hercpetin, Genentech) to tag SK-BR-3 cells. The samples were then processed with the self-assembled magnetic filter to deplete leukocytes and hence enrich tumor cells. SK-BR-3 cells, collected and retained on the membrane filter, were imaged using a fluorescence microscope (Eclipse 80i, Nikon).

Characterization

Magnetic field simulations were used to aid the design and characterization of the self-assembled magnetic filter. The simulated magnetic field strength B is plotted on the cross-section of the self-assembled magnetic filter (Fig. 2a). The magnetic field strength drops rapidly in distance from the surface of the magnetic layer, creating large gradients that lead to strong magnetic forces. The strong gradients of the self-assembled magnet can be seen in contrast to the weak gradients created when the magnetic grains are all aligned in the same direction (Fig. 2b). The simulation geometry was modeled on the self-assembled magnetic filter with 125 μm sized NdFeB dipoles embedded in PDMS, below a 50 μm thick channel of water. The

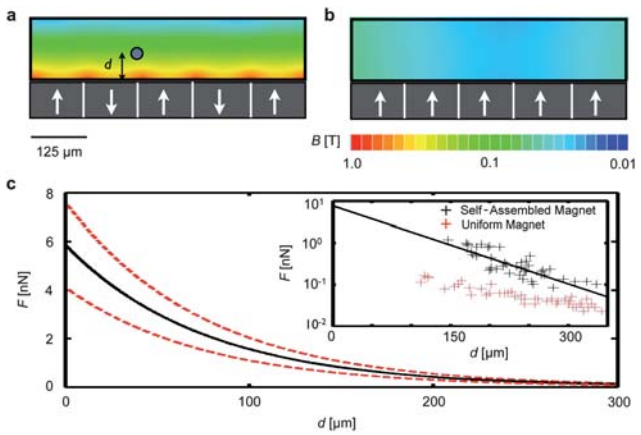

Fig. 2 Characterizing the self-assembled magnet filter. (a) Magnetic field simulations. The magnetic field is plotted on the cross-section of the microfluidic channel for an ideal system of anti-aligned magnetic dipoles. White arrows represent the dipole direction. (b) For comparison, the magnetic field is also plotted for a system in which all of the poles are uniformly aligned. The $|B|$ from (a) decays much faster than in (b), resulting in much greater magnetic forces for the case of anti-aligned dipoles. (c) The inset shows the experimentally measured force on magnetic beads (Dynabead MyOne, Invitrogen) as a function of their distance from a self-assembled magnet (black) and a uniformly magnetized magnet (red). The force measured on the self-assembled magnet has a magnitude of several nN and fits well to an exponentially decay function, plotted (black) with upper and lower bounds (dotted lines in red) *vs.* *d*.

NdFeB material was modeled as being fully magnetized with the saturation magnetization $M_p = 875$ kA m^{-1}. Finite element simulations (Maxwell, Ansoft) were used to find the magnetic field $\boldsymbol{B}$, from which the magnetic forces can be calculated.

The magnetic force, provided by the self-assembled magnetic filter, was measured by optically tracking the motion of magnetic beads (Dynabead MyOne, Invitrogen) in the fluidic channel. The force (F) was calculated by measuring the velocity v of the beads as a function of distance d from the magnet, using Stoke's law ($F = 6\pi\eta r v$); where $\eta = 0.8$ mPa s is the viscosity of the solution and $r = 0.5$ μm is the radius of the bead. The measured force decays exponentially with distance from the magnet's surface (Fig. 2c), agreeing with our model of alternating magnetic dipoles. Furthermore, the magnitude of the force is ~10 nN, which is consistent with the results of numerical simulation, and is >100 times larger than typically found in lithographically patterned magnets.[14,19] A control magnet is constructed, using the same materials as the self-assembled magnet except with the magnetic grains magnetized in the same direction. Using the method described above, the force profile is measured for the control magnet (Fig. 2c). The self-assembled magnet is measured to exert a force >50 times larger than the control magnet, verifying that force enhancement of the self-assembled magnetic filter was indeed due to the anti-parallel arrangement of magnetic dipoles.

Results

The efficiency of the self-assembled magnetic filter was first tested by sorting magnetic beads from non-magnetic polystyrene beads. A suspension that contained 2 μm diameter fluorescent polystyrene beads (Fluospheres F8826, Invitrogen) and 1 μm diameter fluorescent magnetic beads (Dynabead MyOne, Invitrogen) was pumped through the same self-assembled magnetic filter at various flow rates as shown in Fig. 3. As a negative control, identical suspensions were processed using a self-assembled magnetic filter with non-magnetized NdFeB. The change in the composition of the suspension before and after the filtration was quantified by flow cytometry (LSR II, BD Biosciences). Immediately before flow cytometry, samples were spiked with a concentration of polystyrene beads (Fluospheres F8825, Invtorgen) of a third color. The purpose of this "counter bead" was to provide a controlled reference; the composition of non-magnetic and magnetic beads was measured with 10^5 counts of the counter beads. The performance of the self-assembled magnetic filter was gauged using two parameters: *enrichment ratio*: $(C_p^1/C_m^1)/(C_p^0/C_m^0)$ and *recovery ratio*: C_p^1/C_p^0, where $C_p^0$and C_p^1 are the concentration of polystyrene beads before and after sorting respectively, and C_m^0 and C_m^1 are the concentration of magnetic beads before and after sorting respectively.

The results of the bead-sorting experiments are summarized in Fig. 3. The magnetic filter shows a very high capturing efficiency (Fig. 3a and b), enriching the population of nonmagnetic beads by a factor of $>10^5$. The recovery ratio, the fraction of non-magnetic beads that make it through the system, was ~90% (Fig. 3b). In contrast, the negative control, using the non-magnetized NdFeB, showed negligible enrichment (~1). Due to the strong magnetic force, the self-assembled magnetic filter could achieve high capture efficiency even at moderately high flow rates of 1 mL h^{-1}.

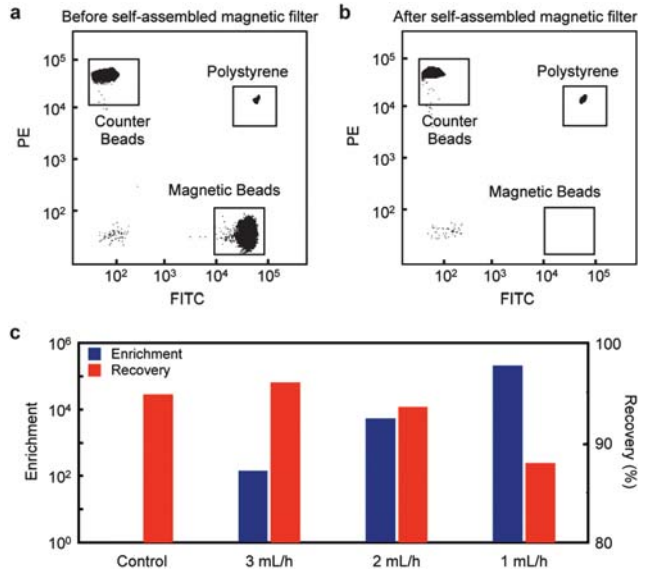

Fig. 3 Characterizing the self-assembled magnetic filter. The self-assembled magnetic filter was tested by filtering a population of magnetic beads from polystyrene beads. Flow cytometry quantified the bead population before (a) and after (b) the filtration. (c) The self-assembled magnetic filter achieves a very high enrichment and recovery ratio, enhancing the population of polystyrene beads to magnetic ones by a factor of $>10^5$ while retaining ~90% of the polystyrene beads. The enrichment and recovery ratio was measured for several flow rates. A control device that has not been magnetized showed no enrichment and a similar recovery rate. The enrichment and recovery ratio was shown to depend on flow rate.

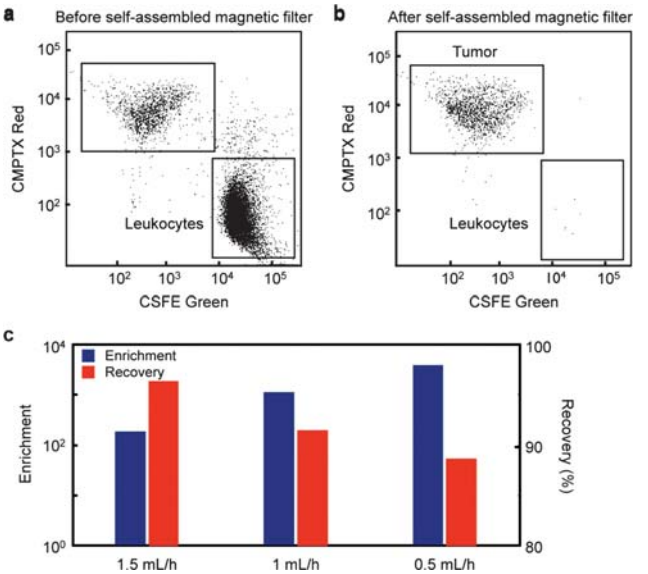

Fig. 4 The self-assembled magnetic filter was demonstrated by filtering a population of leukocytes from tumor cells. (a) shows flow cytometer data of the suspension before filtering and (b) shows it after. The leukocytes were stained green and then tagged with magnetic beads. The tumor cells were stained with a CMPTX red dye. (c) The filter achieves a very high enrichment and recovery ratio, enhancing the population of tumor cells to leukocytes by a factor of $>10^3$ while retaining ~90% of the tumor cells. The enrichment and recovery ratio is shown to depend on flow rate.

The ability of the self-assembled magnetic filter to sort mammalian cells was demonstrated by negatively enriching tumor cells from a suspension of leukocytes that were tagged with CD45 magnetic beads (MACS, Miltenyi Biotec). It is assumed that the targeted CD45+ cells have ~5000 particles per cell.[15] The change in the composition of the suspension before and after filtration was measured by flow cytometry (Fig. 4a). The self-assembled magnetic filter again showed high capturing efficiency, enriching the population of tumor cells to leukocytes by a factor of $>10^3$, outperforming the benchmark system (LD Column, 130-042-901, Miltenyi) which had an enrichment of ~100. The Miltenyi column was tested using the same incubation conditions as the self-assembled magnet, described in the Methods section. The recovery ratio of the self-assembled magnetic filter, the fraction of tumor cells that pass through the system, was ~90%.

The utility of the self-assembled magnetic filter to detect rare cells was demonstrated by repeating the experiment mentioned above, but this time using the single-step incubation and an integrated membrane filter to concentrate the tumor cells for optical inspection. A suspension of tumor cells and leukocytes was incubated concurrently with CD45 antibody conjugated magnetic beads that bind to the leukocytes, and fluorescently labeled antibody that selectively tag tumor cells (Fig. 5a). The suspension was pumped through the self-assembled magnetic filter at 2 mL h^{-1} using a syringe pump to deplete leukocytes and to concentrate tumor cells on the membrane filter at the output port. Fluorescence micrographs of the input and the output are

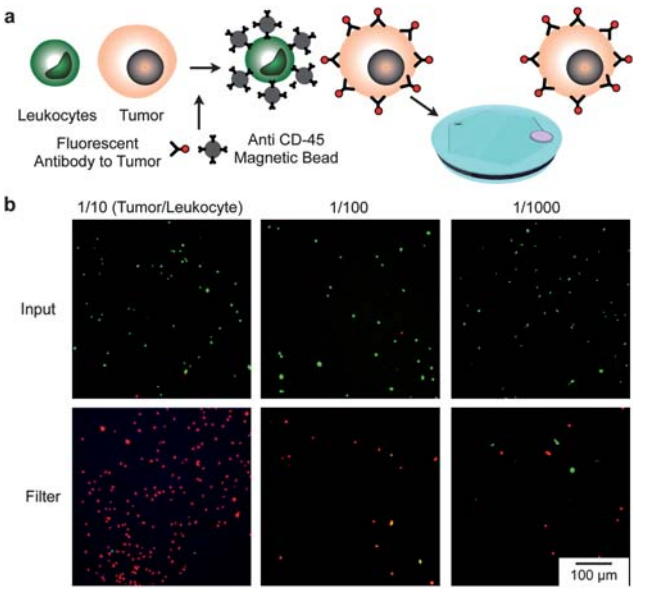

Fig. 5 Detection of rare cells with the self-assembled magnetic filter. (a) A suspension of leukocytes (stained green) and tumor cells were incubated with a mixture of magnetic beads conjugated with anti-CD45 antibodies and fluorescent antibodies to the tumor (anti HER2/*neu*). The suspension was flown through the self-assembled magnetic filter and concentrated on an integrated micropore filter. (b) Fluorescence micrographs of the suspensions before passing through the filter and after concentrated on the micropore filter. The initial concentration of tumor cells to leukocytes was varied from 1/10 to 1/100 to 1/1000.

shown in Fig. 5b for suspensions with initial concentration ratios of 1/10, 1/100, and 1/1000 (tumor/leukocytes). The self-assembled magnetic filter effectively depleted the leukocytes from the suspension, enabling sparse tumor cells to be separated and concentrated for facile detection.

Discussion

We have developed and demonstrated a novel technology for creating strong magnetic field gradients, using the self-assembly of micrometre-sized permanent magnets (NdFeB). We have integrated these strong magnets with a microfluidic channel, and demonstrated that very large sorting efficiencies can be achieved ($>10^5$). These magnets are inexpensive, simple to use, and easy to integrate with microfluidic devices.

In addition to immunomagnetic sorting, there are several applications in which the strong field gradients of the self-assembled magnet can be beneficial. *Clearing bacteria in blood:* the magnet can be combined with high-throughput microfluidics to capture bacteria from whole blood to treat septic patients. The strong forces that our magnet can apply to magnetically tagged bacteria can increase throughput and capture efficiency compared to similar devices that use lithographically patterned magnets.[16] *Magnetofection:* with their simple and planar structure, the self-assembled magnets can be easily integrated with cell culture dish to grow cells on top. The strong, localized field gradients of the self-assembled magnets can attract more magnetic agents to increase transfection efficiency relative to that achieved with external magnets.[24] *Purification of small molecules:* another application for the self-assembled magnets is the purification of small molecules from a biological sample. For examples, magnetic nanoparticles coated to selectively bind to proteins or nucleic acid can be removed with high efficiency using the localized strong magnetic field gradients. The captured molecules then can be released (by cleaving the affinity ligands on the nanoparticles) and enriched to obtain final product of high purity.[25–27] *Fabrication of complex magnetic structures:* the fabrication technique reported here provides a facile way to create magnetic structures of complex geometry to be integrated into microfluidic systems: molds can be patterned of a desired shape and subsequently filled with a mixture of magnetic material and a curable polymer. Such magnets can be used to generate local polarizing fields for various magnetic sensors, including NMR, Hall, and GMR (giant magnetoresistance) devices.

Acknowledgements

The authors gratefully thank R. M. Westervelt (Harvard) for many helpful comments and generous support for the device fabrication through the Center for Nanoscale Systems at Harvard, V. Cortez-Retamozo (MGH) for her help with flow cytometry and for valuable suggestions. We thank Magnequench for its generous support, through the use of their NdFeB magnetic powder. This work is supported in part by National Institute of Health Grants 2R01-EB004626, U01-HL080731, U54-CA119349 and T32-CA79443.

References

1 M. S. Gottlieb, R. Schroff, H. M. Schanker and J. D. Weisman, *N. Engl. J. Med.*, 1981, **305**, 1425–1431.
2 M. Cristofanilli, T. Budd, M. J. Ellis, A. Stopeck, J. Matera, C. Miller, J. M. Reuben, G. V. Doyle, J. Allard, L. Terstappen and D. F. Hayes, *N. Engl. J. Med.*, 2004, **351**, 781–791.
3 D. Mattanovich and N. Borth, *Microb. Cell Fact.*, 2006, **5**, 12.
4 E. Lagasse, H. Connors, M. Al-Dhalimy, M. Reitsma, M. Dohse, L. Osborne, X. Wang, M. Finegold, I. L. Weissman and M. Grompe, *Nat. Med.*, 2000, **11**, 1229–1234.
5 M. Zborowski and J. Chalmers, *Magnetic Cell Separation*, Elsevier, Amsterdam, 2008.
6 S. Miltenyi, W. Muller, W. Weichel and A. Radbruch, *Cytometry*, 1990, **11**, 231–238.
7 S. Nagrath, L. Sequist, D. W. Bell, D. Irimia, L. Ulkus, S. Maheswaran, M. R. Smith, E. L. Kwak, P. Ryan, U. J. Balis, R. G. Tompkins, D. A. Haber and M. Toner, *Nature*, 2007, **450**, 1235–1239.
8 A. Meye, U. Bilkenroth, U. Schmidt, S. Füssel, K. Robel, A. M. Melchior, K. Blümke, D. Pinkert, F. Bartel, C. Linne, H. Taubert and M. P. Wirth, *Int. J. Oncol.*, 2002, **21**, 521–530.
9 J. Oberteuffer, I. Wechsler and P. Marston, *IEEE Trans. Magn.*, 1975, **5**, 1591–1593.
10 D. Melville, F. Paul and S. Roath, *Nature*, 1975, **255**, 706.
11 J. C. Antoine, T. Ternynck, M. Rodrigot and S. Avrameas, *Immunochemistry*, 1978, **15**, 443–452.
12 N. Pamme and C. Wilhelm, *Lab Chip*, 2006, **6**, 974–980.
13 U. Kim and H. T. Soh, *Lab Chip*, 2009, **9**, 2313–2318.
14 H. Lee, A. M. Purdon and R. M. Westervelt, *Appl. Phys. Lett.*, 2004, **85**, 1063–1065.
15 D. W. Inglis, R. Riehn, J. C. Sturm and R. H. Austin, *J. Appl. Phys.*, 2006, **99**, 08K101.
16 N. Xia, T. P. Hunt, B. T. Mayers, E. Alsberg, G. M. Whitesides, R. M. Westervelt and D. E. Ingber, *Biomed. Microdevices*, 2006, **8**, 299–308.
17 J. D. Adams, U. Kim and H. T. Soh, *Proc. Natl. Acad. Sci. U. S. A.*, 2008, **105**, 18165–18170.
18 T. Deng, G. M. Whitesides and M. Radhakrishnan, *Appl. Phys. Lett.*, 2001, **78**, 1775–1777.
19 J. J. Chalmers, M. Zborowski, L. Sun and L. Moore, *Biotechnol. Prog.*, 1998, **14**, 141–148.
20 J. J. Croat, J. F. Herbst, R. W. Lee and F. E. Pinkerton, *J. Appl. Phys.*, 1983, **55**, 2078–2081.
21 G. Vieira, T. Henighan, A. Chen, A. J. Hauser, F. Y. Yang, J. J. Chalmers and R. Sooryakumar, *Phys. Rev. Lett.*, 2009, **103**, 128101–128104.
22 M. Drndić, G. Zabow, C. S. Lee, J. H. Thywissen, K. S. Johnson, M. Prentiss and R. M. Westervelt, *Phys. Rev. A*, 1999, **60**, 4012–4015.
23 R. P. Feynman, *Feynman Lectures on Physics. Volume 2: Mainly Electromagnetism and Matter*, Addison Wesley, Reading, 1964.
24 O. Mykhaylyk, Y. S. Antequera, D. Vlaskou and C. Plank, *Nat. Protoc.*, 2007, **2**, 2391–2411.
25 M. Franzreb, M. Siemann-Herzberg, T. J. Hobley and O. R. Thomas, *Appl. Microbiol. Biotechnol.*, 2006, **70**, 505–516.
26 A. Csordas, A. E. Gerdon, J. D. Adams, J. Qian, S. S. Oh, Y. Xiao and H. T. Soh, *Angew. Chem., Int. Ed.*, 2010, **49**, 355–358.
27 X. Lou, J. Qian, Y. Xiao, L. Viel, A. E. Gerdon, E. T. Lagally, P. Atzberger, T. M. Tarasow, A. J. Heeger and H. T. Soh, *Proc. Natl. Acad. Sci. U. S. A.*, 2009, **106**, 2989–2994.